RAPID SOLIDIFICATION AND HEAT-TREATMENT OF THE $Ti_{92}B_8$ EUTECTIC ALLOY[1]

Gisele Ferreira de Lima[2]
Alex Matos da Silva Costa[3]
Paulo Atsushi Suzuki[4]
Carlos Ângelo Nunes[5]
Gilberto Carvalho Coelho[6]

Abstract
In this work the $Ti_{92}B_8$ alloy was processed via rapid solidification (splat-cooling) and then heat-treated at 700°C and 1000°C. A careful microstructural characterization has shown that after rapid solidification a very fine two-phase microstructure is produced with no significant saturation of B in α/β Ti. There was no indication of amorphous formation in the rapidly solidified splats. Both αTi and TiB are observed in the microstructures of the splats after heat-treatment at 700°C and 1000°C, confirming the stability of the αTi+TiB two-phase region in this temperature range.
Key words: Rapid solidification; Splat-cooling; Eutectic alloy; Ti-B system.

SOLIDIFICAÇÃO RÁPIDA E TRATAMENTO TÉRMICO DA LIGA EUTÉTICA $Ti_{92}B_8$

Resumo
Neste trabalho a liga $Ti_{92}B_8$ foi produzida via solidificação rápida (*splat-cooling*) e em seguida tratada termicamente a 700°C e 1000°C. Uma cuidadosa caracterização microestrutural mostrou que após a solidificação rápida uma fina microestrutura bifásica foi produzida, sem indicação de importante saturação de B em α/β Ti. Não foi encontrado nenhum indício de formação de material amorfo nas amostras solidificadas rapidamente. Foram identificadas as fases αTi e TiB nas microestruturas das amostras produzidas via solidificação rápida após os tratamentos térmicos a 700°C e 1000°C, confirmando a estabilidade do campo bifásico αTi + TiB neste intervalo de temperatura.
Palavras-chave: Solidificação rápida; *Splat-cooling*; Liga eutética; Sistema Ti-B

[1] *Contribuição técnica ao 62° Congresso Anual da ABM – Internacional, 23 a 27 de julho de 2007, Vitória – ES, Brasil.*
[2] *Mestrado em Engenharia de Materiais, Graduação em Engenharia Química*
[3] *Graduação em Engenharia de Materiais (cursando)*
[4] *Doutorado em Física, Mestrado em Física, Graduação em Física*
[5] *Pós-Doutorado em Engenharia de Materiais e Metalúrgica, Doutorado em Engenharia Mecânica, Mestrado em Engenharia Mecânica, Graduação em Engenharia Metalúrgica, Corresponding author: Fax: +55-12-3153-3006, E-mail address: cnunes@demar.eel.usp.br*
[6] *Pós-Doutorado em Engenharia de Materiais e Metalúrgica, Doutorado em Ciência dos Materiais, Mestrado em Engenharia Mecânica, Graduação em Engenharia Metalúrgica*

INTRODUCTION

Due to their low density, high mechanical strength and good corrosion resistance, Ti and Ti alloys are suitable for several important structural applications in the aerospace industry for service in the 700-1000°C temperature range.[1]

The currently accepted Ti-B phase diagram[2] shows in its Ti-rich region the following stable solid phases: αTi solid solution- hcp (at room temperature), βTi solid solution– bcc (885°C - 1670°C) and TiB. An eutectic reaction (L ⇔ βTi + TiB) occurs at 1540°C for ~ 8 at.% B and a peritectoid reaction (βTi + TiB ⇔ αTi) at 885°C.

As part of a work, which aims to evaluate the phase equilibria in the Ti-rich region of the Ti-Si-B system in the 700-1000°C temperature range, it was the objective of this investigation to evaluate the phase equilibria in the Ti-rich region of the Ti-B system in this temperature range. The equilibrium experiments were carried out using samples produced via rapid solidification to allow the attainment of equilibrium conditions. In addition, the microstructure of the rapidly solidified samples also became an interest of this investigation.

The rapid solidification technique used was the splat-cooling method where cooling rates of ~ 10^6 $K.s^{-1}$ are reached.[3,4] Due to the significant undercooling, the solidification conditions lead to a fine-grained microstructure, which assists the attainment of equilibrium in a shorter time. Others possible effects of a rapid solidification process include: solid solution extension, retainment of high-temperature phases, formation of metastable crystalline phases, and formation of amorphous alloys.[5-8] However, all these effects in the microstructure are not only associated to high cooling rates, but they can also depend on the alloy composition, the ratio between the melting temperature and the glass transition temperature, the ratio of the atomic sizes of components and the crystalline structures of the components.[7]

Tavadze[8] studied Ti-B (Ti-rich) alloys prepared by rapid solidification (cooling rate ~ 10^6 $K.s^{-1}$) and observed an extension of the B solubility in Ti and the appearance of an amorphous phase through X-ray diffraction (XRD),[9] however, no details about the method of alloy production was given. Sastry[10] shows that the Ti-1.0B and Ti-1.0C alloys produced via rapid solidification present a large volume fraction of fine dispersoids which increase the yield strength. Other works[11,12] suggest that the solubility of B in both α- and β-Ti may reach values beyond 10 at. % due to rapid solidification.

EXPERIMENTAL PROCEDURE

Initially, an ingot (~ 6g) of the $Ti_{92}B_8$ (at. %) alloy was produced from commercially pure Ti foil (min. 99.3 wt%) and B pieces (min. 99.5 wt%) via arc-melting under a gettered argon atmosphere on a water-cooled copper crucible. Five melting steps were carried out to ensure chemical homogeneity. Samples of ~ 0.1 g were then taken from the ingot and arc-melted just to produce a near spherical shape suitable for levitation in the rapid solidification apparatus. Nine rapidly quenched splats of the $Ti_{92}B_8$ alloy were produced under argon in a Splat-Cooling System from Edmund Bühler GmbH. The steps of levitation, melting and splat-formation were easily accomplished with this alloy composition. Part of the splats were encapsulated under argon in quartz tubes with Ti getter and then heat-treated at 700°C for 120 h and at 1000°C for 48 h. At the end of the experiments the capsules were removed from the furnace and air-cooled. Microstructural characterization of the materials was

performed via X-ray diffraction (XRD) and Scanning electron microscopy (SEM), Conventional and Field-Emission Gun (FEG) using Back Scattered Electrons Detector. The XRD experiments were performed using a Shimadzu model XRD6000 diffractometer at room temperature, using Ni-filtered CuKα (λ = 1,5418 Å) radiation. The arc-melted spherical samples were evaluated in powder form while the splats and heat-treated splats in bulk form (incident X-ray beam in one of the faces). The phases present in the materials were identified by means of comparisons of the experimental diffractograms with simulated diffractograms of the phases using the PowderCell program[13] and crystallographic data.[14] Evaluation of possible solid solution extension was investigated with the refinement of the crystalline structures via the Rietveld method[15] using the FullProf program.[16]

Vickers Microhardness of the produced material was measured using 100 gf load for 30 s, using a MICROMET 2004 Buehler instrument. All the measurements were concentrated in the central region of the samples.

Some evaluation about absorption of penetrating X-rays in the splats were considered in accordance with equation (1),[17] where I = intensity, μ= linear absorption coefficient, μ_m = $\mu\rho$= mass absorption coefficient for each chemical element, ρ = specific mass of the chemical element and t = thickness of X-rays penetration. The mass absorption coefficient of the compounds was calculated with the use of equation (2), where *w* = mass fraction.

$$I = I_0 . \exp(-\mu . t) = I_0 . \exp\left[-\left(\frac{\mu}{\rho} \right) . \rho . t \right] \qquad (1)$$

$$\frac{\mu}{\rho} = w_1 \left(\frac{\mu}{\rho} \right)_1 + w_2 \left(\frac{\mu}{\rho} \right)_2 + \ldots \qquad (2)$$

For the SEM experiments a LEO 1450VP SEM and a Philips FEG-SEM were used. The arc-melted spherical samples were prepared following standard metallographic procedures: hot mounting in resin, grinding in the sequence #220 - # 1000 (SiC sand paper); polishing with colloidal silica suspension (OP-S, Struers). For the splats and the heat-treated splats, cross-sections were observed. They were mounted in cold resin (Epofix Kit, Struers) and prepared by the same metallographic procedures cited above. None of the samples were etched.

RESULTS

The X-ray diffractogram of the arc-melted (sphere) $Ti_{92}B_8$ alloy is shown in Figure 1-a and indicates the presence of αTi and TiB. Figure 2-a shows a SEM (BSE) micrograph of this material where a typical eutectic microstructure is observed, constituted of a αTi (light regions) matrix and TiB particles (dark regions), based on the XRD data and the average atomic number dependence of the SEM image (BSE mode). The TiB particles seem to present a needle-like shape, with higher dimensions such as ~ 30 μm long by ~ 2 μm wide. The lattice parameters of the αTi phase (Table 1) are close to the literature values for pure αTi, a result which does not indicate a large supersaturation of B in αTi after conventional arc melting.

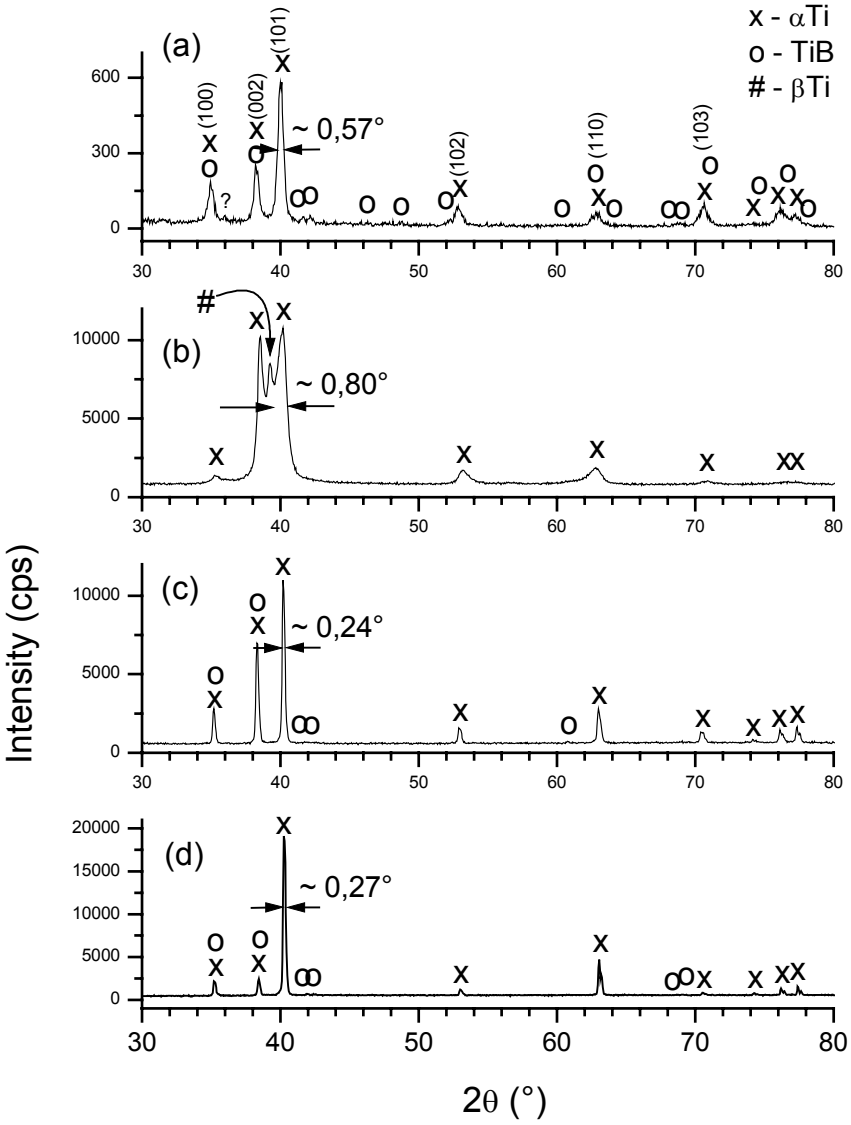

Figure 1 – X-ray diffractograms from the $Ti_{92}B_8$ alloy: (a) sphere – powder form; (b) splat - bulk; (c) splat heat-treated at 700°C for 120 h - bulk; (d) splat heat-treated at 1000°C for 48 h - bulk.

Table 1 – Unit cell parameters of the αTi phase present in the different materials from Rietveld refinement method.

Sample	a (Å)	c (Å)
Pure αTi (Literature [15])	2.9503	4.6810
Sphere	2.950 ± 0.002	4.681 ± 0.006
Splat after rapid solidification	2.952 ± 0.004	4.681 ± 0.001
Splat heat-treated at 700°C for 120 h	2.946 ± 0.001	4.696 ± 0.002
Splat heat-treated at 1000°C for 48 h	2.937 ± 0.003	4.674 ± 0.006

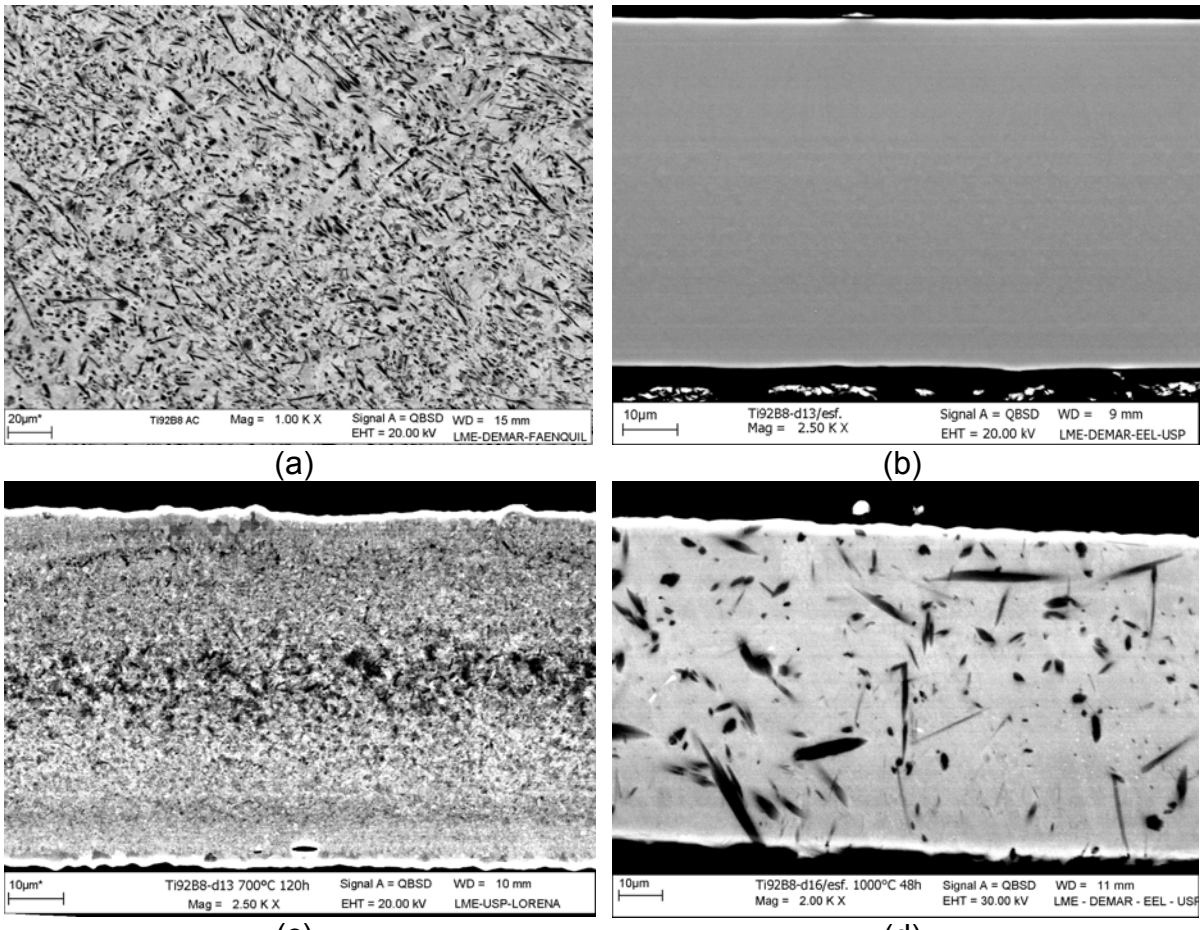

Figure 2 – Micrographs of the $Ti_{92}B_8$ alloy from SEM/BSE: (a) sphere; (b) splat – cross-section; (c) splat heat-treated at 700°C for 120 h – cross-section; (d) splat heat-treated at 1000°C for 48 h – cross section.

The thicknesses of the produced splats were in the range of 53 to 69 μm. Figure 1-b shows an X-ray diffractogram of a splat, which indicates the presence of αTi and possibly some βTi orientated in the [110] direction. The result also suggests a slight orientation of the αTi phase in the direction of the *c* crystallographic axis. The presence of βTi indicates an incomplete βTi → αTi (at 885 °C for pure Ti) transformation due to the high cooling rate achieved in the splat-cooling process.[4, 5,7] Based on our previous observation, the βTi phase should be present only at the regions close to the surface of the splat. In addition, due to possible texture effects and the limited X-rays penetration in the splats, the quantity of the αTi and βTi phases present in the samples cannot be inferred from this diffractogram. The calculated depth of X-rays penetration in the splats for 99% of absorption is almost twice higher than for 90% absorption. According to the calculated values, the scattering of X-rays is just superficial (3 to 10 μm), since the thickness of the splats is ~ 60 μm. The diffractogram in Figure 1-b also shows peaks with the full-width-at-half maximum (FWHM) larger than those in the Figure 1-a, suggesting the presence of finer grains in the microstructure of the splats, as expected. No indication of borides was noted in this difractogram, suggesting a supersaturation of B in (α/β)Ti. However, the lattice parameter of the αTi phase in the splat (Table 1) does not suggest a significant extension of B solid solubility in the αTi phase due to rapid solidification. Figure 2-b shows a SEM (BSE) micrograph from the cross-section of

one splat where the lack of contrast suggests either a very fine boride precipitation or a single-phase microstructure, the latter indicating the formation of a supersaturated solid solution of B in αTi. In order to evaluate this aspect, SEM-FEG (BSE) analyses were carried out and showed a chemical composition contrast as indicated in Figure 3, where the lighter regions are associated to αTi of dimensions smaller than 100 nm. The dark regions in the same figure are associated to a B-rich phase (Ti-poor), however, the nature of this phase could not be determined so far. This type of microstructure was found in the whole cross-section of the splats. Nevertheless, these results indicates that an important quantity of B is not dissolved in the αTi phase and it agrees with the results from the refinement of the αTi lattice parameters which did not suggest a significant extension of B solubility in αTi, and in this way disagrees with the data from the literature.[8,11,12]

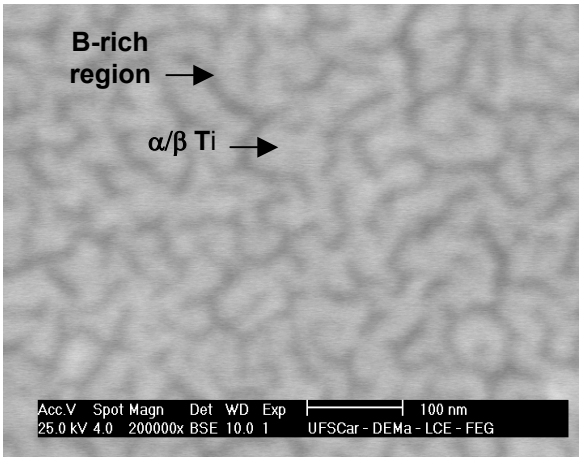

Figure 3 – Croos-section of the $Ti_{92}B_8$ alloy after rapid solidification. Image from SEM-FEG (BSE).

Figure 1-c shows the X-ray diffractogram of a splat heat-treated at 700°C for 120 h. In all splats heat-treated in this condition only the phases αṭi and TiB were identified. The peaks of TiB present low values of intensity and there are no reflections of βTi, indicating the occurrence of the allotropic transformation βTi → αTi during the heat treatment. Comparing the diffractogram of Figure 1-c with the simulated powder difractogram of the αTi phase, it could be observed in the splat a slight orientation in the direction of the *c* crystallographic axis. The Rietveld refinement of the αṭi phase indicated a small change in the *a* and *c* parameters associated to the B presence in the αTi lattice. The Figure 2-c shows a SEM (BSE) micrograph from the cross-section of this splat, the lighter region corresponds to αTi and the dark regions to TiB, with dimensions of ~ 1 or 2 μm. It can be observed a higher amount of TiB in the central part of the splat's cross-section, which leads to a finer grain size of the αTi phase in this region due to grain boundary pinning effects.

Figure 1-d shows the diffractogram of a splat heat-treated at 1000°C for 48 h. As in the previous case, in all splats heat-treated in this condition only the αṭi and TiB phases were observed. Again, the TiB peaks appear with low intensity. The peaks belonging to αTi phase in this diffractogram are narrower (FWHM) than those in the diffractogram of the sphere (Figure 1-a) as well as those in the diffractogram of the splat (Figure 1-b), indicating the presence of larger αTi grains in the heat-treated splat. No reflections of the βTi are observed, however, according to the Ti-B phase diagram,[2] during heat-tretment at 1000°C a βTi+TiB microstructure should be present in the whole sample. After removal of the sample from the furnace, followed

by air cooling, the βTi phase should have transformed to αTi. No significant preferential orientation is observed concerning to the αTi peaks in the diffractogram of Figure 1-d. Also in this case, the lattice parameters of the αTi phase (Table 1) are slightly different from those of the pure αTi phase. Figure 2-d shows a SEM (BSE) micrograph of this splat's cross section. A two-phase microstructure is observed where the dark regions are associated to TiB, confirmed by WDS analyzes (at.% Ti = 52 ± 2 and at.% B = 48 ± 2), and the light regions to αTi. The TiB particles present much larger dimensions than in the previous case, which is clearly associated to the higher temperature and longer time of this heat treatment. The trend for TiB to grow in needle-shape is clearly seen. Moreover, these results from heat-treated (700°C, 1000°) $Ti_{92}B_8$ alloy confirms the stability of the Ti(α/β) + TiB two-phase region in the Ti-rich region of the Ti-B system in the 700°-1000°C temperature range.

Table 2 shows microhardness values from the sphere, splats and heat-treated splats. The highest hardness value of the splat is likely due to its very fine-grained microstructure compared to the others.

Table 2 – Vickers microhardness values of different materials produced in this work.

Sample	Vickers microhardness (HV)
Sphere	255 ± 12
Splat after rapid solidification	443 ± 79
Splat heat-treated at 700°C for 120 h	373 ± 11
Splat heat-treated at 1000°C for 48 h	392 ± 28

SUMMARY

The results of rapid solidification of the $Ti_{92}B_8$ eutectic alloy appointed to a fine and crystalline microstructure. It was not observed the formation of amorphous materials in any of the produced splats. The XRD data of the rapidly solidified splats shows essentially the presence of αTi, and possibly some βTi in the microstructures. It was not observed an important extension of the B solubility in αTi. SEM-FEG (BSE) images of the rapidly solidified splats showed microsegregation of a B-rich phase around the αTi grains. A two-phase microstructures formed by the αTi and TiB phases were formed after heat-treatment of the rapidly solidified splats, confirming the stability of these phases in the 700°C to 1000°C temperature range of the Ti-B system.

Acknowledgments

The authors gratefully acknowledge Capes and FAPESP (# 01/09529-7) for financial support.

REFERENCES

1 DESTEFANI, J. D. Introdution to Titanium and Titanium alloys. In: **ASM International Handbook: Properties and Selection: Nonferrous Alloys and Special-Purpose Materials.**10ed.,Vol. 2, USA: ASM International, 1990. p. 586 - 591.

2 MASSALSKI, T. B. et al. Boron-Titanium. In: **Binary Alloy Phase Diagrams**, Metals Park: ASM, 1990. p. 544 - 548.

3 DUWES, P.; WILLENS R. H., KLEMENT jr.,W. J. **Appl. Phys.** v. 31, p. 1136, 1960.
4 PREDECKI, P.; MULLENDORE, A. W.; GRANT, N. J. A Study of the Splat Cooling Technique. **Transactions of the metallurgical society of AIME**, vol. 233, p. 1581 – 1586, 1965.
5 DAS, S. K. High performance materials by rapid solidification processing. In: MOHANTY, O. N.; SIVARAMAKRISHNAN, C. S. **Rapid Solidification Processing and Technology.** Jamshedpur, India: National Metallurgical Laboratory, v. 38, 39, 1989. p. 1 - 20.
6 ANOSHKIN, N. F.; DEMCHENKOV, G. G. Material science and technological aspects of rapid solidified titanium alloy production. **Materials Science and Engineering,** v. A243, p. 263 - 268,1998.
7 KOCH, C.C. Rapid Solidification of Intermetallic Compounds. **International Materials Reviews**, vol. 33, n. 4, p. 201 – 219, 1988.
8 TAVADZE, G. F.; OKROSTSVARIDZE, O. Sh.; TAVADZE, F. N.; TASAGAREISHVILI, G. V.; MAZMISHVILI, G. A. Crystallization of eutectic system Ti-B, V-B, Zr-B, and Hf-B at ultra-high rates of cooling. In: **7th International Symposium on Boron, Borides and Related Compounds**, June9-12, 1981, Sweden, Uppsala. Abstract. p.368.
9 MURRAY, J. L.; LIAO, P. K.; SPEAR, K. E. The B-Ti (Boron-Titanium) System. In: Murray, J. L. **Phase Diagrams of binary titanium alloys.** USA: ASM international, 1990. p. 33 – 38.
10 SASTRY, S. M. L.; PENG, T. C.; MESCHTER, P. J.; O'NEAL J. E. Rapid solidification processing of titanium alloys. **Journal of Metals**, 1983.
11 WHANG, S. H. Rapidly Solidified Titanium Alloys for High Temperature Applications. **Journal of Mat. Science.** v. 21, n. 7, p. 2224 - 2238, 1986.
12 FAN, Z.; MIODOWNIK, A. P. The young's moduli of in situ Ti/TiB composites obtained by rapid solidification processing. **Journal of Materials Science,** v. 29, p. 1127 – 1134, 1994.
13 KRAUS, W.; NOLZE, G. J. Powder Cell – a program for the representation and manipulation of crystal structure and calculation of the resulting X-ray powder patterns. **J. Appl. Cryst.**, vol. 29, p. 301 – 303, 1996.
14 Villars, P.; Calvert, L.D. Pearson's Handbook of Crystallographic Data for Intermetallic phases. 2nd. **ASM International**. Materials Park: 1991, 4v.
15 RIETVELD, H. M. **J. Appl. Cryst.**, 2, p. 65 – 71, 1969.
16 RODRIGUEZ-CARVAJAL, J. **Reference Guide for the Computer Program FullProf.** Saclay, France: Laboratoire Leon Brillouin, CEA-CNRS, 1996.
17 KLUG, H. P.; ALEXANDER, L. E. X-Ray diffration procedures for polycrystalline and amorphous materials. 2ed. **Wiley-Interscience Publication**. New York: 1974.